STRUCTURE FUNCTION STUDIES ON A LIPID BINDING PROTEIN H7 FROM VACCINIA VIRUS.

By

LINYI TANG

Bachelor of Science in Biology Science

South China Normal University

Guangzhou, China

2010

Submitted to the Faculty of the
Graduate College of the
Oklahoma State University
in partial fulfillment of
the requirements for
the Degree of
MASTER OF SCIENCE
July, 2016

STRUCTURE FUNCTION STUDIES ON A

LIPID BINDING PROTEIN H7 FROM

VACCINIA VIRUS.

Thesis Approved:

Dr. Junpeng Deng

Thesis Adviser

Dr. Robert Matts

Dr. Andrew Mort

Dr. Haobo Jiang

Name: LINYI TANG

Date of Degree: JULY, 2016

Title of Study: STRUCTURE FUNCTION STUDIES ON A LIPID BINDING PROTEIN H7 FROM VACCNINA VIRUS.

Major Field: BIOCHEMISTRY AND MOLECULAR BIOLOGY

Abstract: H7 as a member of the recently identified viral membrane assembly proteins (VMAPs) plays a key role in poxvirus membrane biogenesis. Although the detailed manner of the poxvirus membrane biogenesis remains largely unclear, it is suggested that H7 works together with other VMAPs to facilitate the acquisition of membrane from the host's endoplasmic reticulum (ER). In eukaryotes, phosphoinositides and their binding proteins have been known for their importance in membrane and protein trafficking. From our previous study, a phosphoinositide-binding site was identified on two regions of the H7 protein, including the C-terminal tail and a surface patch that is comprised of basic residues. Through lipid overlay and fluorescence polarization-based lipid binding assays, the binding of H7 with phosphoinositides, PI3P and PI4P, was confirmed. A model, in which a positively charged pocket for binding phosphoinositdes was formed by two regions interacting with each other and the C-terminal's possible function serving as a switch, was proposed from the previous structure-function studies. Yet due to the intrinsic nature, the 29 residues at the C-terminal tail were not visible in the published H7 structure. In this study, we aim to solve the complete structure of H7 in complex with phosphoinositides PI3P, PI4P. Due to the lack of sequence homology of H7 to proteins outside the poxvirus family, the structure-function study of H7 with lipid can provide a novel perspective into the detailed mechanism of poxvirus membrane biogenesis.

TABLE OF CONTENTS

Chapter Page

LIST OF TABLES

LIST OF FIGURES

Figure Page

CHAPTER I

INTRODUCTION

I.1 Poxvirus

Poxvirus is a large family of viruses that can affect both human and animals. There are four genera of poxviruses that can contribute to human infectious: orthopoxvirus, parapoxvirus, yatapoxvirus, molluscipoxvirus (Condit, Moussatche, & Traktman, 2006). The symptoms of poxvirus infection normally involve skin nodules, formation of lesions or disseminated rash. Smallpox, which is under the orthopoxvius category, might be one of the best-known poxvirus-related diseases. Although in 1979 the WHO had acclaimed its eradication through the vaccine campaign, pathogenic orthopoxviruses remain a dangerous threat to the public health. Orthopoxviruses include variola virus, monkey pox virus and vaccinia virus (VACV) In the U.S., routine smallpox immunization was discontinued in the early-1970s. As a result, the current U.S. population is highly susceptible to smallpox that may be re-introduced maliciously or accidentally. Our studies will provide important clues to the controlling mechanism for poxvirus host tropism and fundamental knowledge for further improving VACV-based vaccine vector for infectious diseases and cancer.

Vaccinia virus is a prototype of poxvirus. It was used as an active agent in the eradication of smallpox. It is what we are using in the laboratory environment to understand the mechanisms of poxvirus's morphogenesis.

I.1.1 Poxvirus Structure

Poxvirus are enveloped, brick shaped virions that are normally 200 nm in diameters and 300 nm in length (Condit et al., 2006).

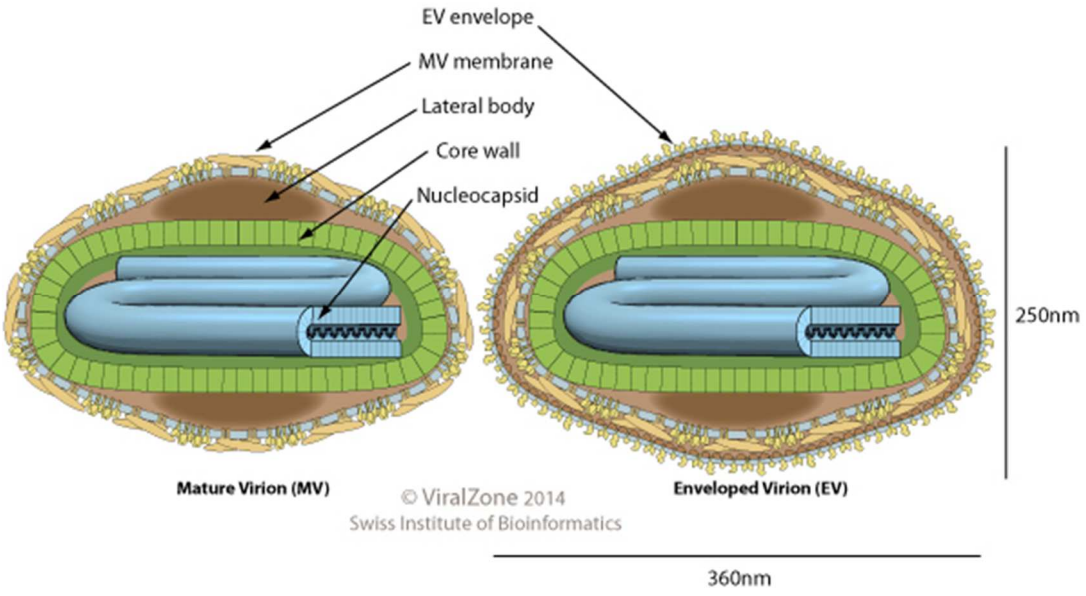

Figure1.1 Poxviridae structure model (Swiss Institute of Bioinformatics)

The extracellular enveloped virus (EEV) and intracellular mature virus (IMV) (Figure 1.1) are both infectious. Compared to IMV, the EEV form of the virus has an extra membrane outside which is the envelope. The poxvirus envelope at early stage is a single membrane lipid bilayer that is stabilized by a honeycomb lattice coating, which later on can be completely replaced by a paracrystalline coating with the development of the virion (Heuser, 2005). Within the envelope and membrane, there is a "dumbbell" shaped core, containing nucleic acid encased by the core wall. The lateral body, of which the function is not quite clear, occupies the space between the membrane and the core.

I.1.2 Poxvirus Genetics

The poxvirus genome, normally ranging from 130 to 375 kb, is encased in the core of the virus (Condit et al., 2006). As a family of large cytoplasmic virus, one of the most unique and important features of poxvirus is that they replicate and transcribe their large, double stranded DNA genome in the cytoplasm instead of in the nucleus region of the infected cells. It is a rather complex and distinguishable process since all the enzymes needed for the replication and transcription have to be encoded completely in the cytoplasm of the host cell at the right time, in the right place. Specific sites whereas virus's replication and transcription occurs in the cytoplasm are called "**viral factories**". These "viral factories" are also sites where viral assembly happens following the viral genome replication. The machinery of this intricate process involves the viral genome's interaction with the microtubules (MTs) and endoplasmic reticulum (ER) of the host cell in the beginning of viral invasion (Ward & Moss, 2001).

I.1.3 Poxvirus Morphogenesis

In general, poxvirus morphogenesis is a rather complicated process (Figure 1.2). As the phrase "cycle " indicate, the end point is also a new beginning---the poxvirus life cycle starts with its two infectious forms of its final products, i.e. the mature virus (MV) and extracellular enveloped virus (EEV).

MV and EEV are structurally, antigenically and functionally distinguishable.(McFadden, 2005). Their membrane fusion with the host cell is the starting of the viral entry. The exact manner of the viral entry is not understood. Yet, it is clear that once the virus entered, both MV and EEV will release its genome-containing core to the infected cell's cytoplasm. Upon release of the core, an early viral transcriptional mechanism is to be function. This mechanism ensures that proteins that are crucial for the subsequent steps in the life cycle are synthesized right away in the infected cell's cytoplasm. These early proteins will facilitate t1) the core "un-coating"; 2)

the release of the parental DNA; 3) viral DNA replication (McFadden, 2005; Roberts & Smith, 2008). After all early preparations for the viral invasion is finished, the virus will express 'intermediate' and 'late stage' genes in its genome as different sets of proteins that for use in the following steps.

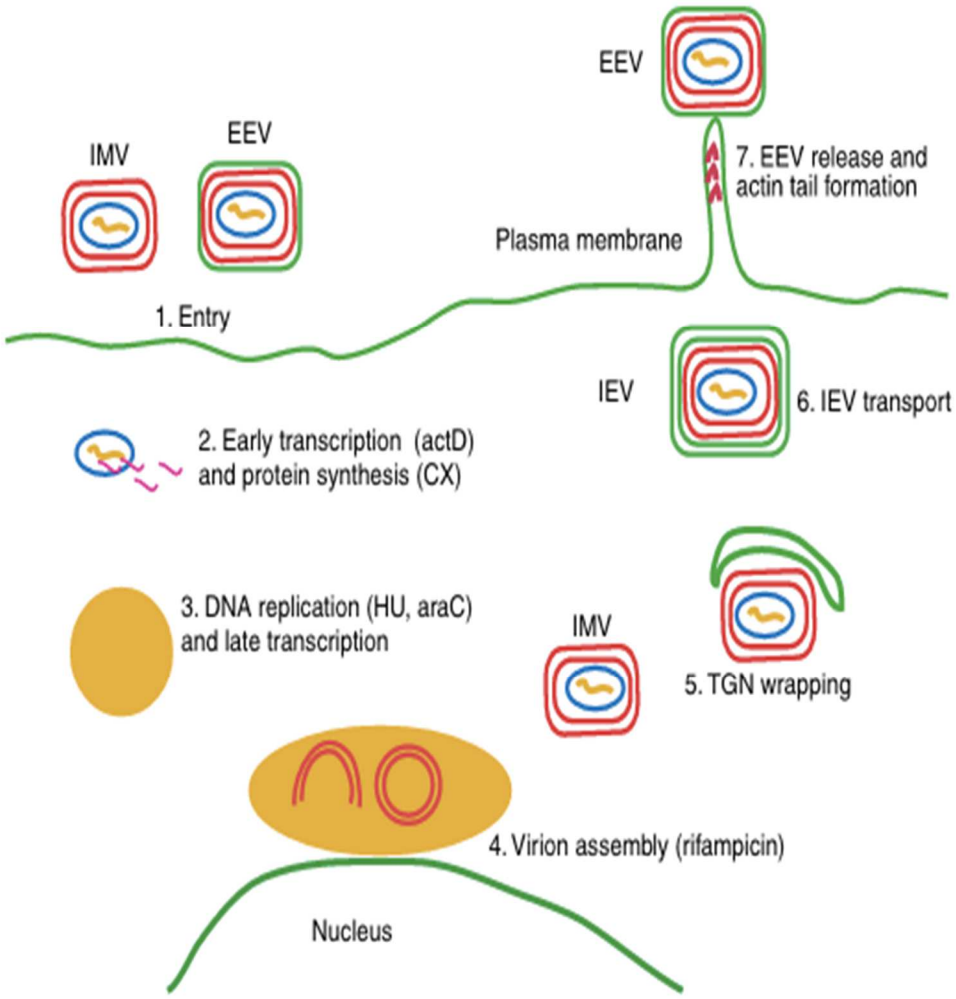

Figure1.2 Schematic of vaccine virus life cycle. (Schramm & Locker, 2005)

The viral assembly starts with the formation of a unique open-ended membrane structure—crescent shaped membrane. This membrane serves as a scaffold for the later

assembling process. A spherical immature virion (IV) that lacks the viral genome appears next.. Only until the IVs take up the viral DNA, forms the first infectious form of the virus----- intracellular mature virus, IMV.. Some of these newly formed IMVs stay at these sites while others travel outside of these 'viral factories'. These IMVs 'travellers' move to a 'transportation center' or microtubule-organizing center. From there, a small percentage of IMVs are wrapped by membranes derived from the Golgi network or endosomes. When the transformation is done, a new name is given to this small percentage of IMVs-----intracellular enveloped virus (IEV). IEV will then utilize or hijack the infected cell's 'transportation system'----microtubules and kinesin travel to cell's surface (Ward & Moss, 2001). After arrive at the cell surface, the virus envelope forms by fusing its outer membrane with the host cell's plasma membrane. The enveloped virus can stay or release to the medium through budding. The released enveloped virus is the other infectious form of poxvirus mentioned at the beginning of this section, called extracellular enveloped virus (EEV). To this step, the life cycle of poxvirus is completed (McFadden, 2005; Roberts & Smith, 2008).

I.3 Phosphoinositides

Phosphoinositides are phosphorylated phosphatidylinositol (PI). There are three phosphorylation sites on the inositol ring of PI, the hydroxyl-groups on the 3^{rd} ,4^{th} 5^{th} positions of the inositol ring. Through reversible phosphorylation by different kinases, 7 different PIs are generated (Figure 1.3), PI3P, PI4P, PI5P, PI (3,4) P, PI (3,5) P, PI (4,5) P and PI (3,4,5) P (Di Paolo & De Camilli, 2006). The distribution of these 7 phosphoinositides in different subcellular membranes is distinct and therefore contents of phosphoinositides in membranes can be used to identify organelles (Balla, 2013; Di Paolo & De Camilli, 2006).

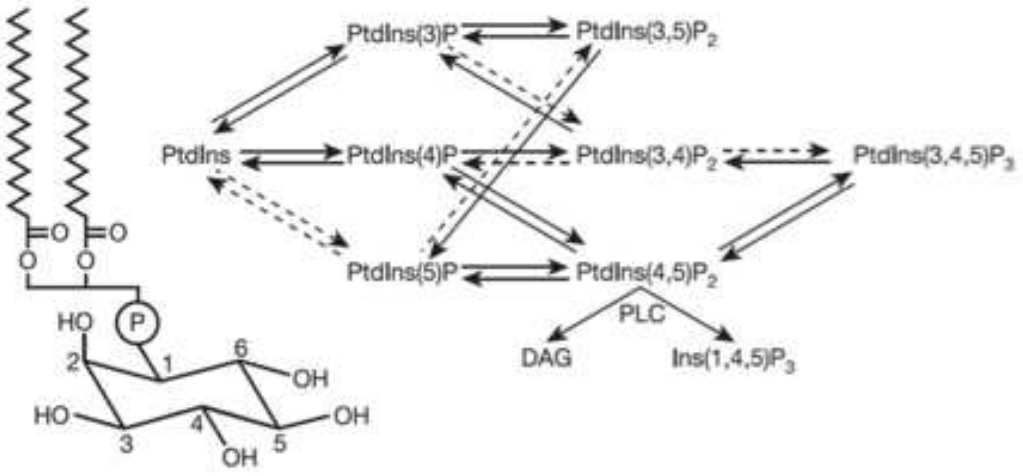

Figure1.3 Generation of seven phophoinositides from phosphatidylinositol (PtdIns)

(Di Paolo & De Camilli, 2006)

Although phosphatidylinositol only composes less than 15% of the total phospholipids in cells, they have a major impact on cell biology. Their phosphorylated forms—phosphoinositides, play important roles in mediating cell signaling pathways, membrane trafficking, plasma membrane-cytoskeleton interactions, etc. (Di Paolo & De Camilli, 2006). The physiological functions of phosphoinositides are largely determined by the inositol head group's interaction with different PI kinases and phosphatases. The negatively charged inositol head groups can bind specific proteins through electrostatic interactions, this in turn, expands the functions of phosphoinositides in cells.

I.4 Phosphoinositides Binding Proteins

Effector proteins specifically bind with phosphoinositides through electrostatic interaction. They contain one of the following domains: PX (phox- homology), PH (plexkstrin homology), FYVE (Fab1p/YOTB/Vac1p/EEA1), ENTN (Espin N-terminal homology) (Lorizate & Krausslich, 2011). Among all the phosphoinositdes, PI3P normally binds with endosomal proteins like EEA1, Hrs and SARA that contain either PX or FYVE domains (Figure

1.4.Stenmark & Gillooly, 2001). Effector proteins harboring PH and ENTN domains are the primary PI4P binding modules and mostly found in the Golgi apparatus (Delang, Paeshuyse, & Neyts, 2012). The binding with phosphoinositides will induce conformational changes of these effector proteins and thus result in protein's allosteric regulation.

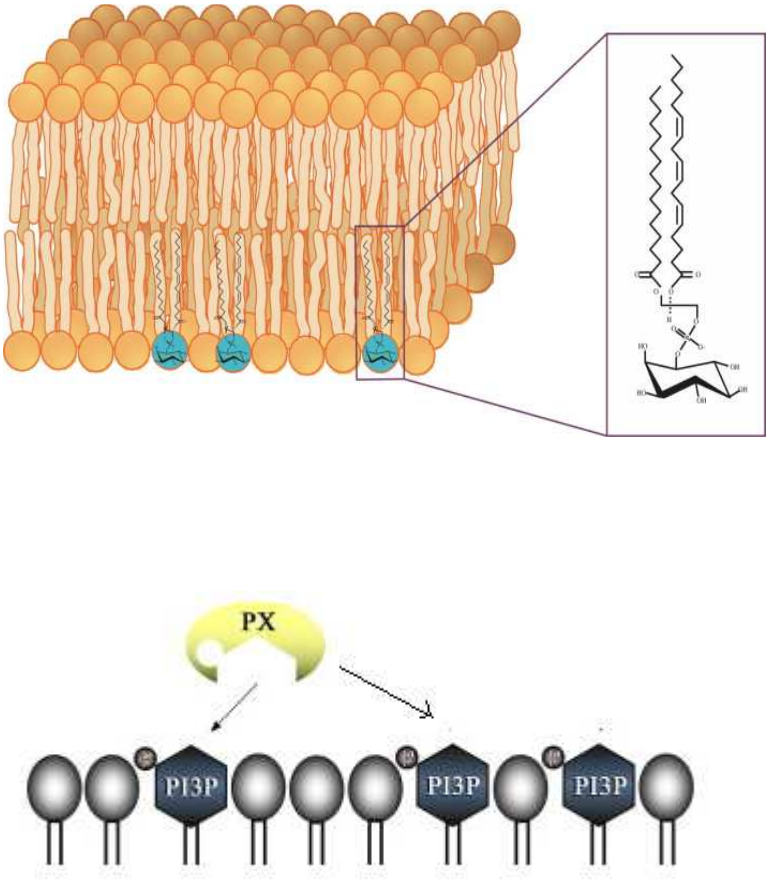

Figure 1.4 Schematic of PX domain bind with PI3P

(Progress in lipid research, Volume 50 issue 1)

I.5 Protein Crystallization and X-ray Crystallography.

Protein crystallization is a process of crystallizing the protein of interests. Gene cloning and protein engineering are almost always engaged to get the protein. Different protein purification techniques such as nickel affinity chromatography, HPLC, ion exchange etc. are utilized to purify the protein to a homogeneous status. After a highly purified and concentrated protein sample is obtained, the next step is to set the protein of interest for crystallization. Briefly, it is the process of testing out buffer conditions under which protein can be crystallized. There are normally three ways of preparing the crystal: hanging drop method, sitting drop method or micro-dialysis. The sitting drop method is what we are using in the lab. After a protein crystal is obtained, crystal optimization and selenomethionione replacement are normally applied before setting the crystal for X-Ray crystallography (Wlodawer, Minor, Dauter, & Jaskolski, 2008).

X-Ray crystallography it is used to study protein structure at the atomic level after the protein crystal is obtained. Figure 1.6 shows major steps involved in X-Ray crystallography.

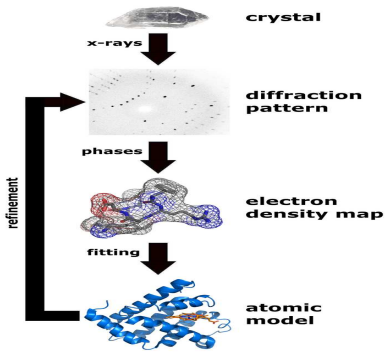

Figure 1.5 Workflow of Solving the Molecule Structure by X-Ray Crystallography. (wikipedia)

This complicated process can be briefly understood as, firstly using a high energy beam (X-Ray) to focus on the crystal (the subject), then a diffraction pattern of the crystal's electrons will appear on a image plate (like shadows on the wall) and can be recorded. While this diffraction pattern contains useful information of all atoms in the crystal, it is not enough for deciphering the crystal structure. X-ray, like other electro-magnetic radiations, it has both particle and wave properties. The diffraction pattern only give information on its particle (amplitude) side, the wave side as being called phase is missing. This is the well-known phase problem in the X-ray crystallography. Thus at this point, selenomethionione or heavy metal replacement methods will be introduced to obtain information for solving the phase problem. After obtaining the atoms information from both amplitude and phase side, the electron density map can be calculated and interpreted into an atomic model. A model of the protein structure will be build using computer programs. An R-factor, which represents the difference between the data and the model, of 25% or less is expected for the final version of the model (Wlodawer et al., 2008).

CHAPTER II

LITEREATRUE REVIEW

Vaccinia virus (VACA) as a prototype of poxvirus has been actively studied over the last decades. Despite the tremendous success of the WHO-led small pox vaccine campaign using vaccnia virus as an active agent in the late 1970s and lots of continuous studies, the detailed mechanisms of vaccnia virus morphogenesis remains largely unclear.

Taking a closer look into the VACA life cycle (section **I.1.3**), one might find nature's perfect illustration on the philosophy---"less is more" and be amazed by how complicated and precise the life processes are carried out by such a simple structure. Indeed, as one simple structured and genetically unique virus that replicates and transcribes its whole genome in the cytoplasm of the infected cell, VACA has evolved lots of elegant strategies to manipulate its host cells in facilitating its "invasion" at all stages. For example, one of the ways the virus uses to enter the host cells is by mimicking the apoptotic host cells thus triggers endocytosis (Amara & Mercer, 2015); in terms of facilitating the viral replication, the host cell's innate immune pathways are suppressed through the virus induced up-regulation of the anti-inflammatory cytokines (Liu et al., 2005) the heat shock response of the infected cells is shut off or differently regulated with the VACA infection (Liem & Liu, 2016); to ensure viral translation, the VACA hijacks the host cell's translation machinery by manipulating the PI3P/AKT signaling pathway during the infection (Liem & Liu, 2016; McNulty et al., 2010), etc.

With technological advances in molecular and structural biochemistry, people's understanding of different molecular mechanisms involved in those strategies has been largely improved. Among all the aspects of the complicated VACA morphogenesis, the **viral membrane biogenesis** remains to be the least understood. Following the viral replication, the formation of an open-ended membrane structure---crescent membrane is the first step of the viral assembly process. The structure and origin of the crescent membrane has been a long debate among researchers over the last half-century. Contradictory theories (Dales S Fau - Mosbach & Mosbach, 1968; Higashi, Ozaki, & Ichimiya, 1960), in terms of the structure --- whether it is one membrane or two distinct layers, have been aroused. The controversy ended with the advances in the imaging techniques, confirming the crescent membrane is a single membrane of honeycomb lattice comprised of VACA D13 protein trimmers (Heuser, 2005; Szajner, Weisberg, Lebowitz, Heuser, & Moss, 2005). In view of the crescent membrane formation, rather than synthesized "*de novo*" (Dales S Fau - Mosbach & Mosbach, 1968), more evidence (Chlanda, Carbajal, Cyrklaff, Griffiths, & Krijnse-Locker, 2009; Husain, Weisberg As Fau - Moss, & Moss, 2006; Krijnse Locker, Chlanda, Sachsenheimer, & Brugger, 2013) support that the viral membrane is derived and ruptured from ER by a highly controlled mechanism.

In this highly controlled membrane biogenesis mechanism, several viral proteins have been identified for their crucial roles in the membrane formation. Essential structural proteins for crescent membrane formation are the scaffold protein D13 and the two major trans-membrane proteins A14 and A17 (Erlandson et al., 2016; Liu, Cooper, Howley, & Hayball, 2014). Regulatory proteins that are fundamental for viral membrane assembly are termed as **viral membrane assembly proteins (VMAPs)**.

Up to date, there are five identified VMAPs: A6, A11, A30.5, H7 and L2. Other than L2---the early-transcribed membrane protein that is co-localize with the ER throughout the whole replication process and is also found in the crescent membrane (Maruri-Avidal, Weisberg, &

Moss, 2011), the rest of VAMPs are exclusively expressed after the genome replication with different locations preference. Conditional lethal inducible and deletion mutants were applied in studying the roles of individual VMAPs. With pieces of information pulling together, **models of VACA crescent membrane formation** have been proposed in several recent reviews/publications (Liu et al., 2014; Meng, Wu, Yan, Deng, & Xiang, 2013; Moss, 2015). The premise in these models is that there are constant breaks generated in the ER. Although the exact manner of how the breaks in the ER are generated remains unclear, it is suggested that, as shown in Figure 2.1 (Liu et al., 2014), in the viral infection, L2 associates with the ER membrane and recruits the ER membrane segments to the viral factory, then L2 interacts with A30.5 (a protein that co-localize with ER and L2 but is synthesized after the DNA replication.) and A11 (a protein that is expressed late in the infection and is only localized in the viral factories.) or possibly some other unidentified proteins to stabilize the ER membrane segments by capping the free end of the segments. The structural viral membrane proteins D13, A17 and A14 are detected on the ER segments in the viral factories. They are thought to interact with each other and serve as precursor for elongating the segments to form crescents and spherical immature virions by fusion with additional ER membrane segments. However, further studies are needed to attest and complete the above assumptions.

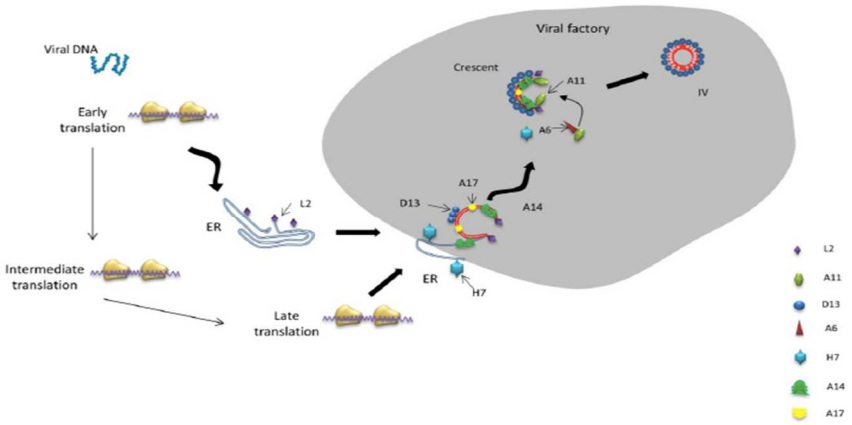

Figure 2.1 Model of Vaccinia virus crescent membrane formation

Among all the VMAPs, the 17k Da **H7** protein is the focus of this study. Previous mutant deletion studies demonstrated that H7 is crucial for crescent membrane and IV formation (Meng et al., 2013; Satheshkumar, Weisberg, & Moss, 2009). However, similar to A11, it yet shares no sequence homology, H7 does not integrate into the subsequent MV membrane. Also, studies showed that H7 localizes not only in viral factories but also throughout the cytoplasm, indicating its function is not limited to viral factories (Satheshkumar et al., 2009). Structure –function studies previously done by our lab (Kolli et al., 2015) shed some lights into the possible function of H7 from a structural perspective.

In the published paper, the majority of the H7 protein structure has been solved. A phosphoinositide-binding site was identified on two regions of the H7 protein, including the C-terminal tail and a surface patch that is comprised of basic residues. Through lipid overlay and fluorescence polarization-based lipid binding assays, the binding of H7 with phosphoinositides, PI3P and PI4P, was confirmed. A model, in which a positively charged pocket for binding phosphoinositdes was formed by two regions interacting with each other, the C-terminal's possible function serving as a switch, was proposed from the study. Yet due to the intrinsic nature, the 29 residues at the C-terminal tail were not visible in the published H7 structure in the absence of lipids.

In this study, we aim to solve the complete structure of H7 in complex with phosphoinositides PI3P and PI4P. Since H7 shares no homologs outside the poxvirus family and there is no discernible functional motif identified, the structure-function study of H7 with lipid can provide a novel perspective into the detailed mechanism of poxvirus membrane biogenesis.

.

CHAPTER III

METHODOLOGHY

III.1 Protein Expression in *E.coli*

Table 1. Buffers and Media Formulation for protein expression in *E.coli*

1. 1L LB Media	2. 1000X IPTG
5g NaCl	Dissolve 2.38g IPTG into 10ml ddH_20
5g Yeast Extract	3.1000X Antibiotics
10g Tryptone	Kanamycin: 50mg/ml
Add ddH_20 to 1L.	Ampcilin: 100mg/ml

1.Prepare LB media media and autoclave for 45 minutes on liquid cycle. Afterwards, inoculate 50-100 ml LB media with fresh antibiotic, using glycerol stock cells. Incubate the culture at 30 °C, 250 rpm overnight as the overnight culture.

2. Spin down the overnight culture using a sterilized tube by centrifugation (Beckman centrifuge), 3500 rpm for 20 minutes. After the centrifugation, use pipette to gently re-suspend the cell pellet in fresh media (use 1:50 dilution factor as 50ml overnight culture can be used for 2 liter large scale expression) with fresh antibiotics. Incubate the large scaled cell culture at 37°C, at 250 rpm. Monitor cell growth by measuring OD_{600} using the spectrophotometer. When OD_{600} reaches 0.6-0.7, adjust the shaker's temperature to 18 °C. Allow at least 45 min for the cells to cool down completely before inducing. When the OD_{600} reaches around 1.0, spike 1ml IPTG in to each 1L flask to initiate protein overexpression. Lower the temperature to 18°C and shake at 250 rpm for overnight.

3. Harvest the overnight cell culture by centrifugation at 4000rpm, 30 minutes. After centrifugation, transfer the cell pellet into a new, sterilized 50ml falcon tube. If not proceeding to the purification step, the cell pellet are stored at -20°C.

III.2 Protein Purification

III.2.1 Two-step Ni-Column Purification (For protein with His-tags)

Table 2. Buffers for protein purification

1.Buffer A: 20mM Tris, 500mM Nacl, 10% glycerol, 20mM Imidazole, pH8.0
2.Buffer B: 20mM Tris, 500mM Nacl, 10% glycerol, 250mM Imidazole, pH8.0
3.Dialysis Buffer: 20mM Tris, 500mM Nacl, 10% glycerol, pH8.0

1. Add lysozyme to a finial concentration of 0.5mg/ml into Buffer A, Re-suspend the cell pellet from the final step of protein expression in buffer A, using 35-50 ml Buffer A per 1 L culture. Leave the suspended cell pellet on ice or 4 °C for 40 minutes.

2. To reduce the viscosity, add DNAase (5mg/ml in ddH_20, use 5-10 ul for 50ml lysate) in the cell lysate.

3. Use Cell Homogenizer to further lyse the cells.

4. Centrifuge (Sorval) the cell lysate at 11,000 rpm, 4 °C for 30 minutes.

5. Filter the cell supernatant by using a 0.45 um filter.

6. Pre-equilibrated Ni-NTA resin (Qiagen) buffer A. Incubate the filtered supernatant with Ni-NTA resin on rocker in the cold room, rocking for 1 hour. (Binding capacity: 1ml resin for 10 mg protein.)

7. Use a 25 ml gravity flow column to collect the Ni-NTA resin, allowing all the liquid to flow through.

8. Wash the resin with 100 ml cold buffer A.

9. Elute the protein out with 20 ml buffer B and collect the flow in a 50 ml falcon tube.

10. Measure the protein concentration by Bradrad regent. Add a proper amount of rTEV (Qiagen) protease into the protein sample for cleaving the N-terminal 6xHis tag. Use 1:40 molar ratio of TEV: protein sample. The Molecular weight of rTEV is around 30KDa.

11. Put the mixture in a dialysis bag and subject to 1L dialysis buffer at 4 °C in cold room overnight. Clean the Ni-NTA column with 50 ml buffer B and then 30 ml buffer A.

12. Equilibrate the Ni-NTA column from previous steps with 30 ml dialysis buffer. Filter the dialyzed protein sample with 0.45 um filter and let it flow through the column 3 times by gravity flow. Collect the flow through. This is the purified protein. Run SDS-PAGE gel for protein analysis.

III.2.2 Size Exclusion Chromatography

To further purify the target protein after Ni-Column purification, use AKTA HPLC system (GE Health) and highload 16/600 superdex 75 column (GE Health) to separate the target protein from impurity based on the difference of molecular sizes. Generally, the higher the molecular weight of the protein, the earlier the peak appears on the chromatography.

III.2.3 Ion Exchange Chromatography

Table 3. Buffer in Ion Exchange Chromatography

Buffer A: 50mM Nacl, 20mM Tris, pH 8.0
Buffer B: 1M Nacl, 20mM Tris, pH8.0

Use AKTA HPLC system (GE Health) and Q sepharose column (GE Health) to separate molecular base on their different binding affinity with the column under a certain pH and with a gradient salt concentration.

III.2.4 High Pressure Chromatography

Use AKTA HPLC system (GE Health) and s200 high-pressure column (GE Health) to separate molecular with a higher resolution.

III.3 Protein Concentration Assay

Use the Bio-Rad protein assay kit (Life research). The detailed steps refer to the product instruction online.

III.4 Lipid Overlay Assay

1. Block the PIP strip (Echelon Biosciences) in 10ml 3% BSA, TBS-T (Tris buffered saline and Tween 20) for 1 hour at room temperature, shake gently during the blocking.

2. Discard the blocking buffer from step1, add protein of interest into 3% BSA, at final concentration of 1ug/ml, incubate with the PIP strip for 1 hour at room temperature, shake gently during the incubation.

3. Discard the solution from step2, wash the PIP sheet with TBST, 5ml, 5 minute each time, 6 times.

4. Incubate the PIP sheet with mouse polyclonal anti-H7 antibodies (provided by Dr.Xiang from UTHSCSA) at 1:1000 ratio at room temperature for 1 hour.

5. Wash the PIP sheet as in step3.

6.Incubate the PIP sheet with anti mouse secondary HPR antibody at 1:2000 ratio at room temperature for 1 hour.

7. Wash the PIP sheet as in step3.

8. The signal was detected by chemiluminescence (West Pico by Thermo Scientific).

III.5 Crystallization

Sitting-drops method was used for the crystallization. Crystallization screening plates were set up manually or by Gryphon LCP (Art Robins Instrument) with 0.5ul protein+0.5ul screening buffer in the well and 50ul screening buffer in the reservoir, at both room temperature and 4 degree.

The 96-well commercial crystallization screens used in the study are listed in Table 7.

Table 4. Crystallization screens used in the study

Screen	Manufacturer
PEG/Ion (I/II)	Hampton Research
Index	Hampton Research
WIZARD (I/II/III/IV)	Rigaku Reagent
Crystal	Hampton Research
JCSG Core (I/II/III/IV)	Qiagen
NATRIX	Hampton Research
WIZARD Precipitant Synergy	Rigaku Reagent

For the H7 lipid complex, lipid PI3P and PI4P are prepared in 50mM Hepes, pH 7.0 buffer at 10mM stock concentration. In the complex, the lipid final concentration is 1mM. Thus, 45ul H7+5ul lipid stock, incubate in cold room for 1 hour. When adding lipid and protein together, add lipid first to avoid local high concentration.

CHAPTER IV

RESULTS

III.1 H7 Construct Sequence Information

III.1.1 H7 BamB Construct Sequence Information

Apo H7 crystals diffracted to about 2.7Å resolution. In order to explore different crystal forms of H7 that offer better resolution, we used a fusion strategy to clone H7 into a modified pET vector containing *E.coli* BamB gene (Jansen, Baker, & Sousa, 2015) with a N-terminal removable His tag. Two different linkers between BamB and H7 were designed giving PBO99: N-His- (TEV site)-BamB-G-S-H7, and PBO100: N-His- (TEV site)-BamB-G-S-G-S-H7. The rationale was BamB could promote diverse crystallization since BamB itself crystalized in multiple crystal lattices (www.rcsb.org).

PBO99: N-His- (TEV site)-BamB-G-S-H7

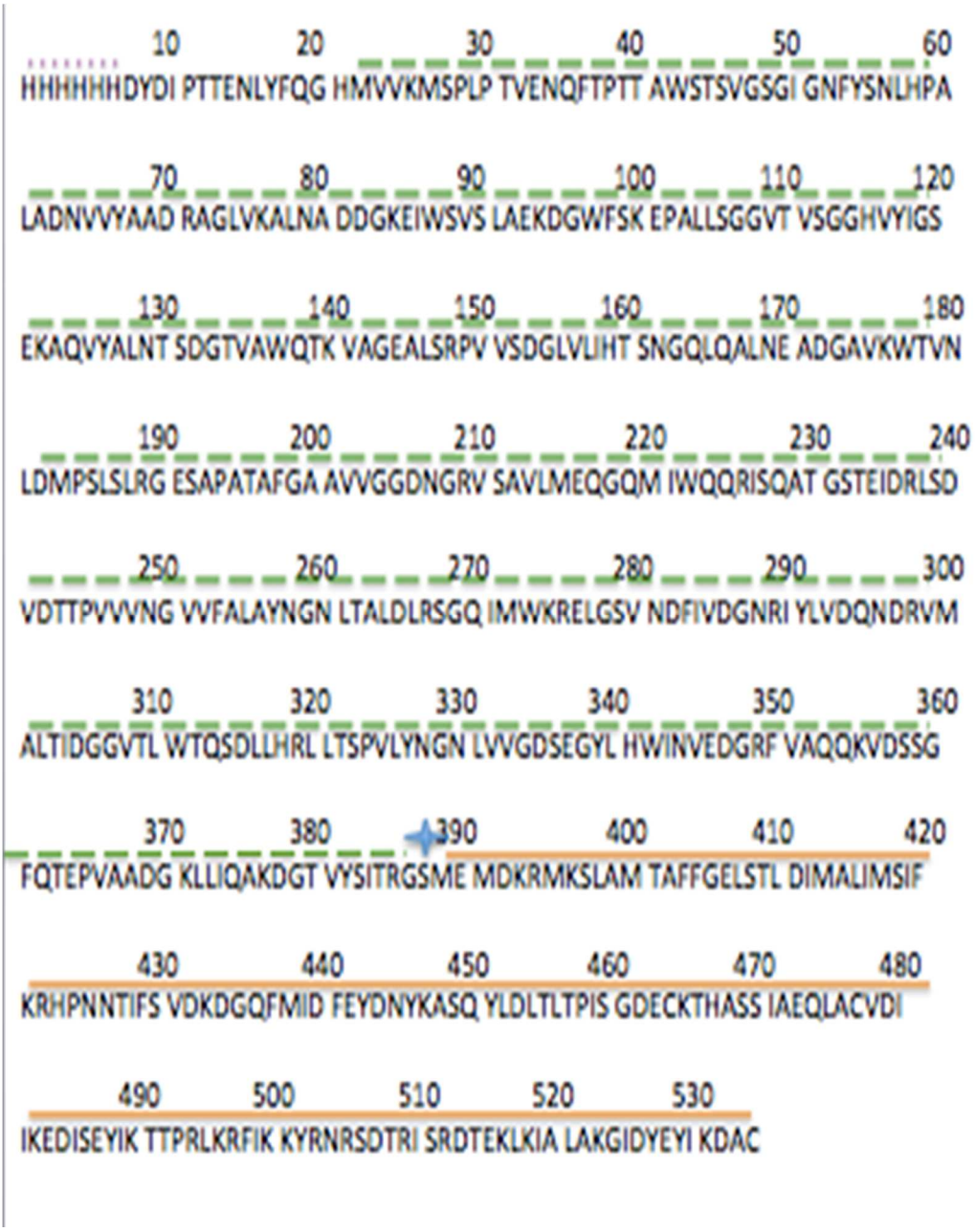

The 6XHis tag is labeled by the dot, the green dash line labels the BamB protein, while the ‘star’ indicates the G-S linker, H7 protein itself is indicated by the straight line.

PBO100: N-His- (TEV site)-BamB-G-S-G-S-H7

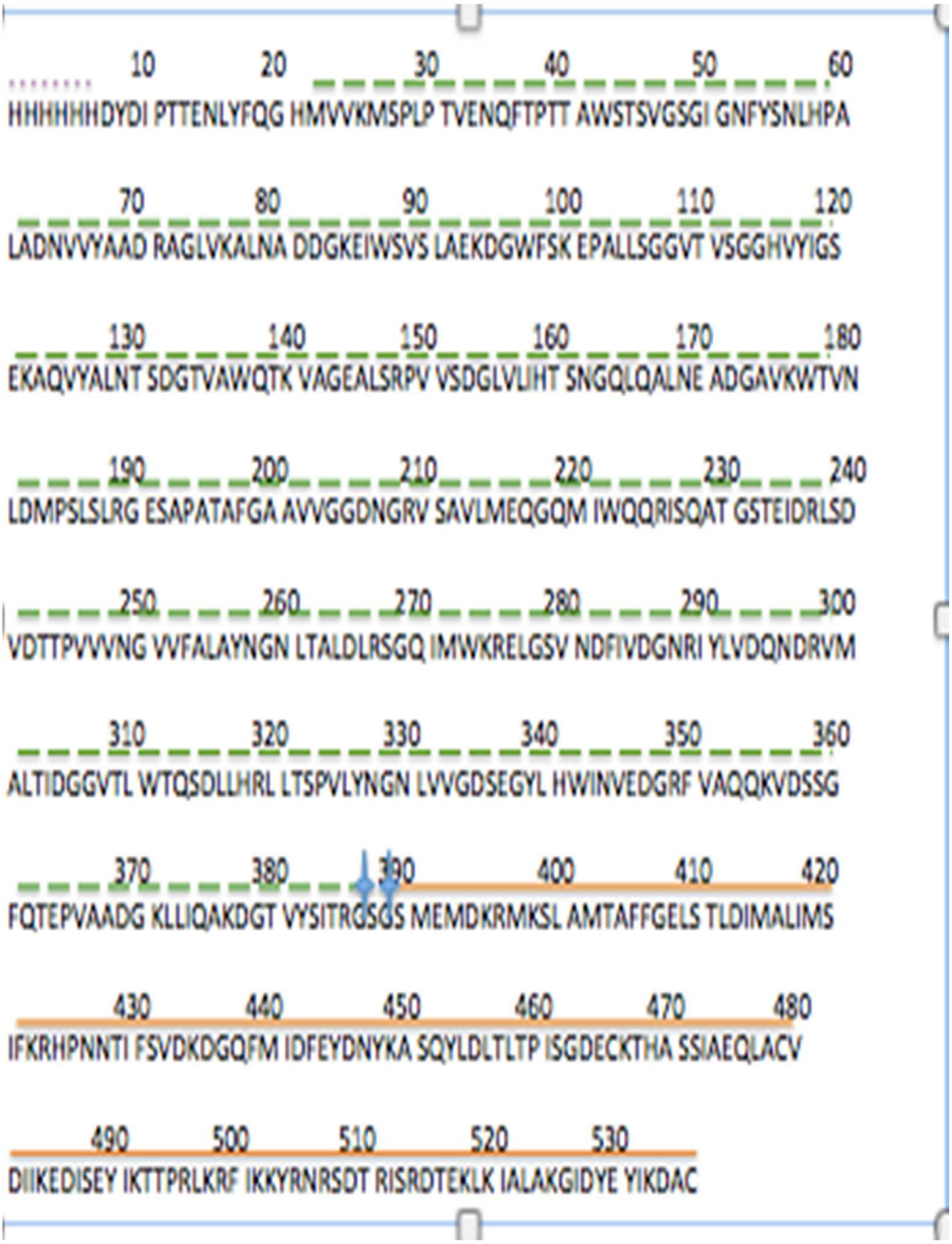

The 6XHis tag is labeled by the dot, the green dash line labels the BamB protein, while the ‘star’ indicates the G-S-G-S linker, H7 protein itself is indicated by the orange straight line.

H7 BamB constructs are started with a 6-His tag following with a TEV enzyme site. A BamB protein was fused to the H7 protein with a G-S (for PBO99 construct) or G-S-G-S (for PBO 100 construct). The isoelectric point (PI) and molecular weight (MW) for both constructs with and without His tag are summarized in the Table 5 below.

Tabel 5. H7 BamB constructs PI and MW

	Theoretical pI	**MW**
99:N-His-BamB-GS-H7	5.28	58.6
100:N-His-BamB-GSGS-H7	5.3	59
99:BamB-GS-H7	5.08	56
100:BamB-GSGS-H7	5.08	56
BamB	4.73	39

III.1.2 H7 Sumo Construct Sequence Information

In parallel, we hypothesized that lipid binding with H7 could stabilize its flexible C-terminal tail, generating high-resolution diffracting crystals. Therefore, we continued to purify the Apo H7 protein as published method and used for co-crystallization with PI3P and PI4P.

H7-SUMO construct: N-His-SUMO-H7

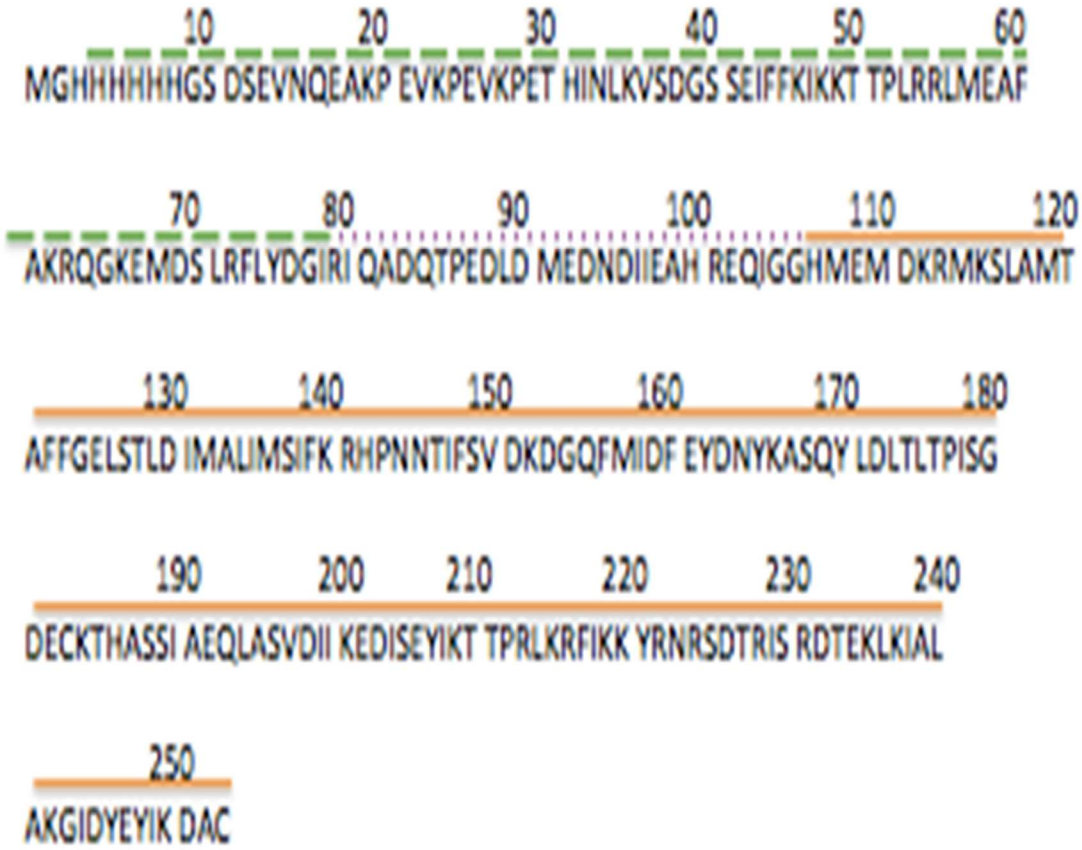

H7 SUMO construct starts with a 6-His-SUMO moiety followed with the sequence of H7. The long dash line labels the His-SUMO, while the dots label the ULP1 enzymatic site, the orange straight line labels the H7 protein itself. The isoelectric point (PI) and molecular weight (MW) for the H7 SUMO constructs with and without His tag are summarized in the Table 6 below

Tabel 6. H7 SUMO construct PI and MW

	Theoretical pI	MW (kDa)
H7SUMO:N-His-SUMO-H7	6.0	29
H7	6.74	17
N-His-sumo	5.81	12

III.2 H7 Construct Expression and Purification

III.2.1 H7 BamB Construct Expression and Purification

The H7 BamB constructs were expressed with 0.2mM IPTG induction at 18°C overnight. A 2-step Ni-NTA affinity purification was applied for the initial purification. The first Ni-NTA purification step captures his-tagged BamB-H7 fusion. After TEV cleavage of the his-tag moiety, the untagged BamB-H7 fusion was applied on the 2nd subtracting Ni-NTA column and collected as flow through (Fig. 3.1). The expression and Ni-NTA purification protein samples were collected at each step for a SDS-PAGE gel analysis. The result is presented as follows:

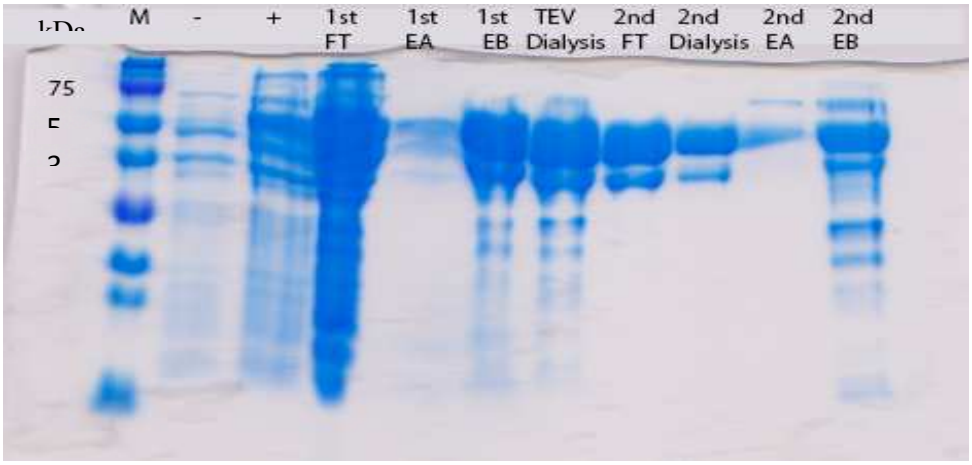

Figure 3.1 2-Litter H7 BamB construct expression and 2-Step Ni-NTA purification.

(The lanes from left to right indicate: protein marker, non-induce sample, IPTG induced sample, cell lysate flown through Ni-NTA resin, 1st buffer A elution, 1st buffer B elution,)

The final product that contains the target protein BamB-H7 is majorly in 2nd FT section.

After 2nd Ni-NTA purification, protein concentration for:

PBO99 (H7 BamB with a shorter linker) is 2.5mg/ml, total: 25-30mg, the productivity for this construct is around 15mg/L in *E.coli*.

PBO100 (H7 BamB with a longer linker) is 2.7mg/ml., total: 25-30mg, the productivity for this construct is around 15mg/L in *E.coli*.

After the two- step Ni-NTA purification, the 2nd FT section sample was collected and concentrated for further purification by Highload 75 column in AKTA HPLC equipment. The purification chromatography is as followed.

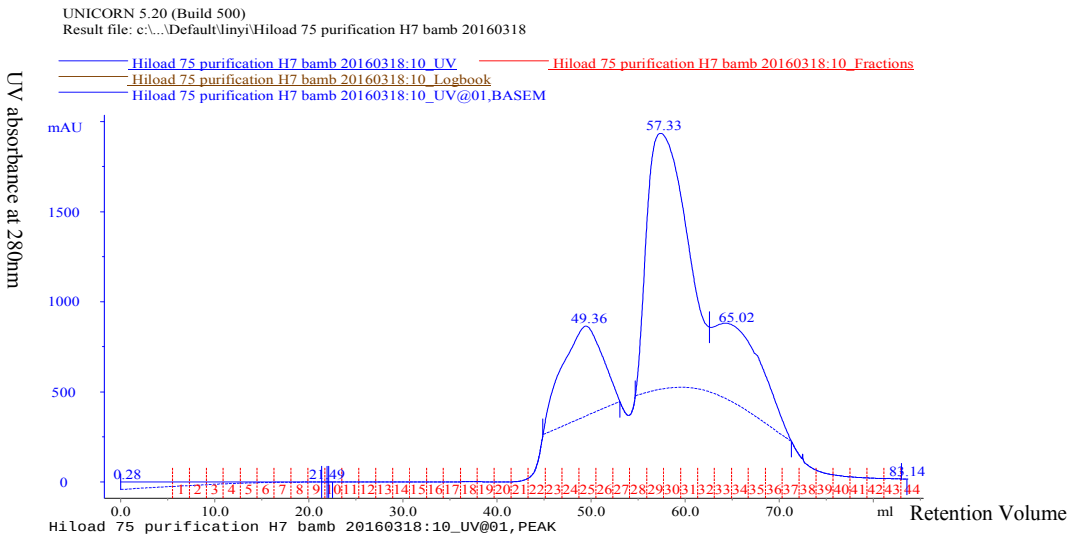

Figure 3.2 Gel filtration chromatography of H7 BamB on superdex hi-load 75 column

To verify the proteins contained in each peak, a 10% SDS-PAGE gel was applied. The result of the SDS-PAGE gel is as follows:

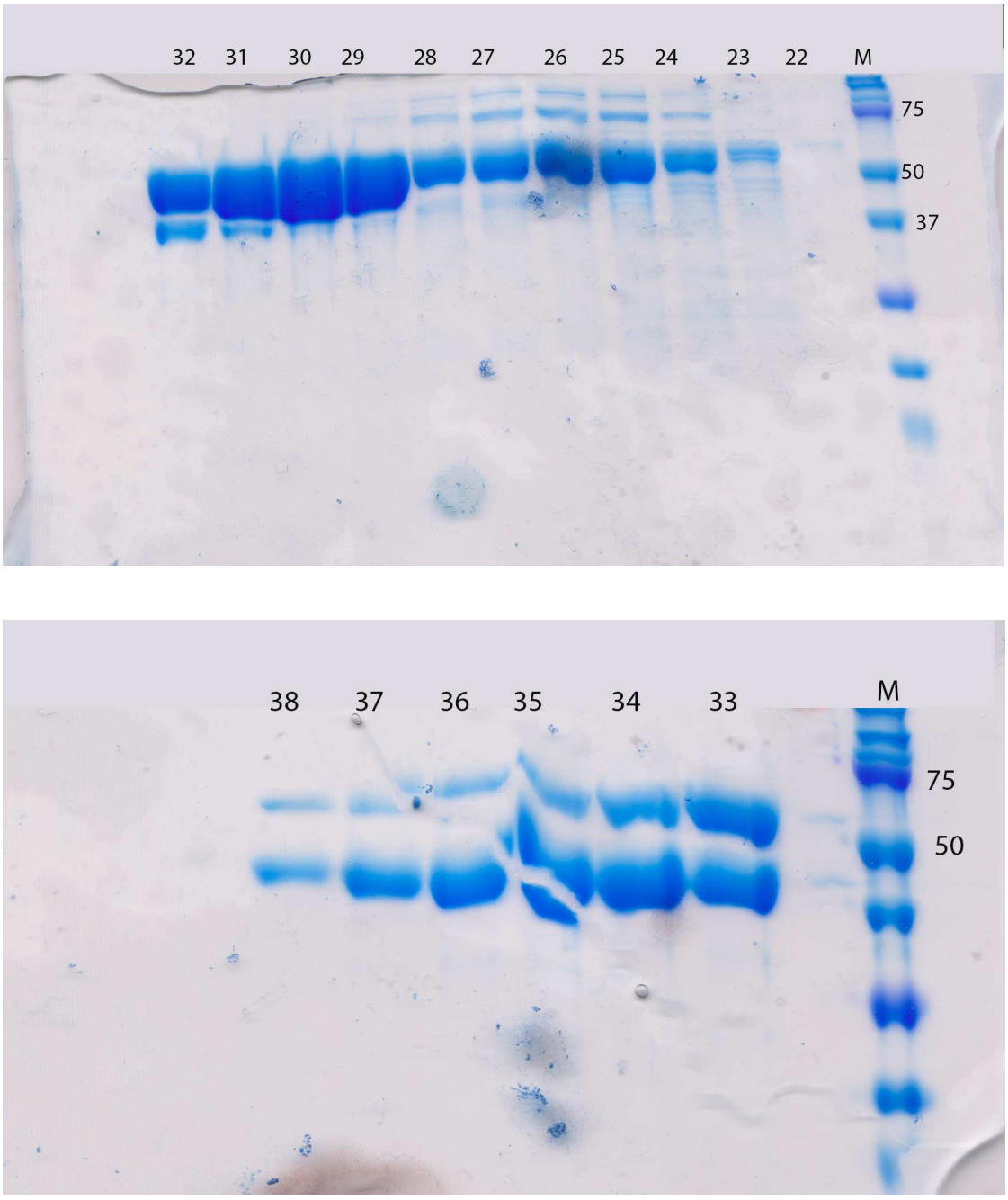

Figure 3.3 SDS-PAGE analysis of H7 BamB from fractions of gel filtration

("M" refers to the protein marker; Fraction 22 to27 refers to leftist peak, fraction 28 to 32 refers to the middle peak and fraction 33 to 38 refers to the rightest peak)

From the SDS-PAGE gel's result on the H7 BamB construct's Highload 75 chromatography, we collected fraction 29 to 32 which bands molecular weight are close to 56 k Da to do some further purification by high pressure column s200. One of the results (since all of the fraction runs have the same chromatography, here only present one as an example.) from the high-pressure s200 analytics column is as follows:

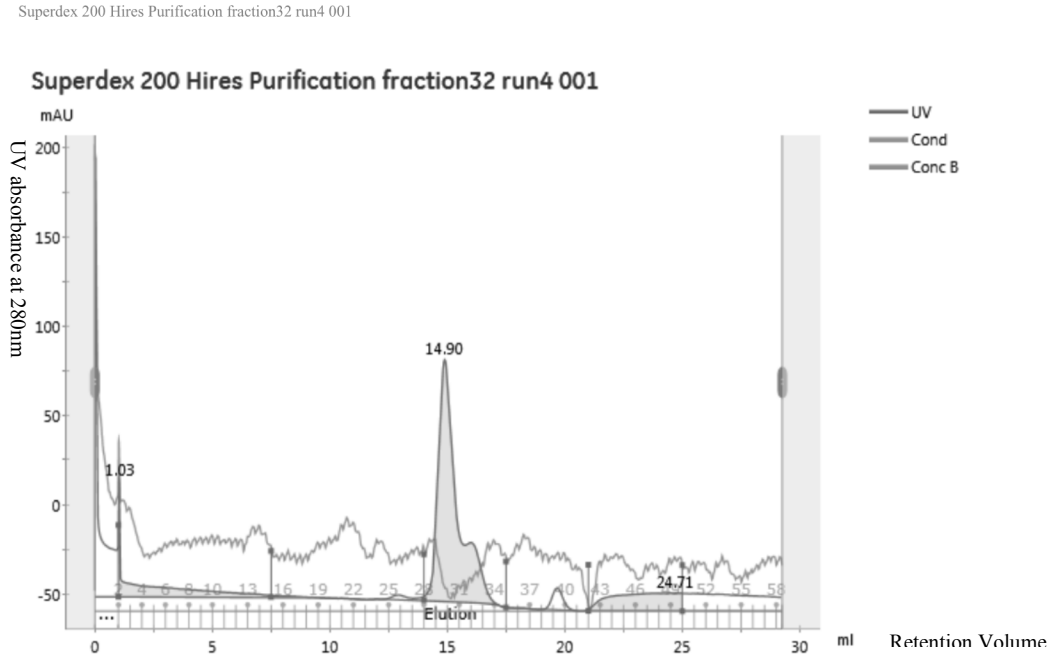

Figure 3.4 H7 BamB construct high-pressure column chromatography.To verify the contents of the peak appeared on the chromatography, a 10% SDS-PAGE gel was applied. The SDS-PAGE gel result on this is presenting as follows:

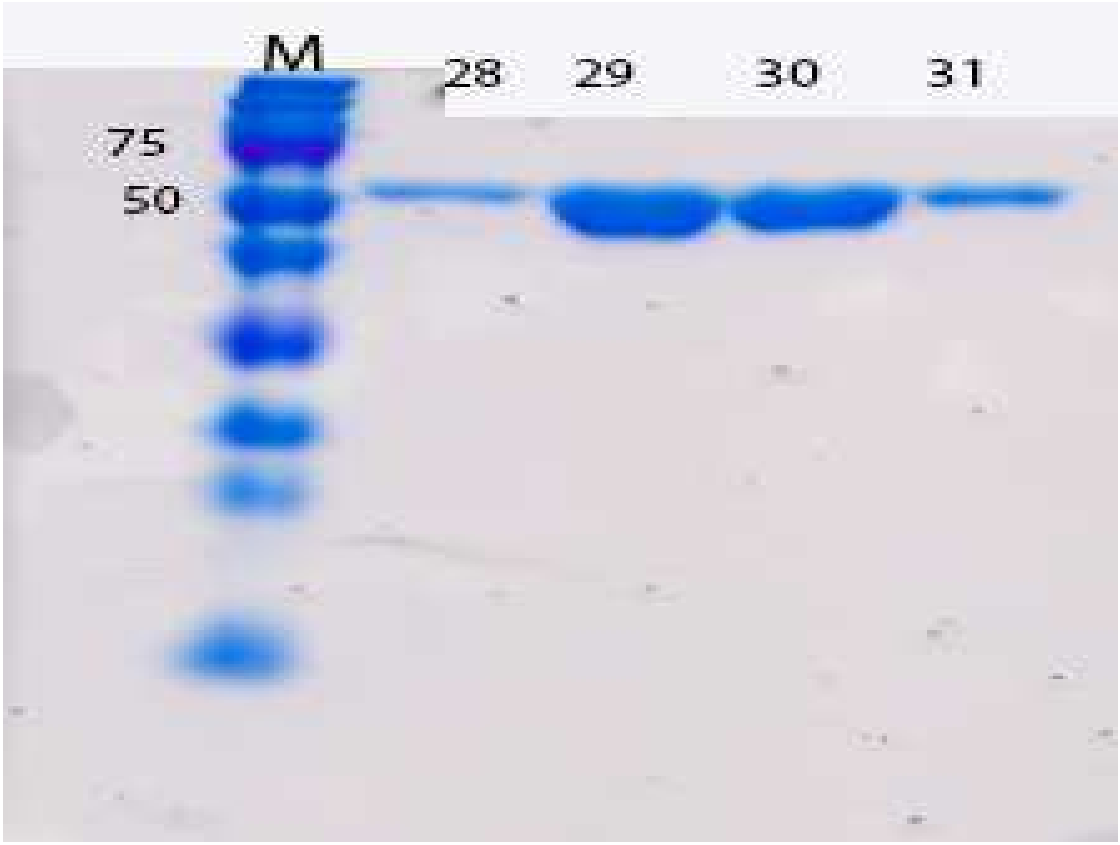

Figure3.5 SDS-PAGE analysis of H7 BamB collected from gel filtration chromatography using high-pressure s200 column.

("M" refers to the protein marker; Fraction 28 to 31 refers to the peak on the high pressure s200 column chromatography.)

From the SDS-PAGE gel's result on the the H7 BamB construct High-pressure 200 column chromatography, we collected all the fractions that only contains one single band with the molecular weight around 56k Da to concentrate them to a saturation point and ready for crystalllizatioon set up.

To verify the pufity of the protein sample after concentration, a 10% SDS-PAGE gel was applied. The final product that used for crystallization on the SDS-PAGE gel is presenting as followed:

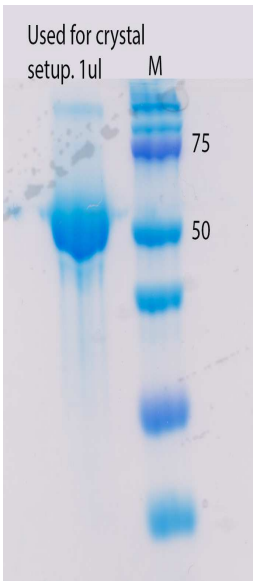

Figure 3.6 SDS-PAGE analysis of H7 BamB final product.

("M" refers to the protein marker.)

The purified H7 BamB protein was concentrated to around 10mg/ml in 20 mM Tris, 50mM Nacl, flash frozen in LN2 and stored at -80 ℃ until usage for crystallization and lipid binding overlay assay.

III.2.2 H7 SUMO Construct Expression and Purification

The H7 SUMO constructs were expressed with 0.2mM IPTG induction at 18ºC overnight. A 2-step Ni-NTA purification strategy was used for the initial purification as described in III.2.1. Protein samples along the expression and Ni-NTA purification steps were collected and analyzed on a SDS-PAGE experiment. The result is presented as following:

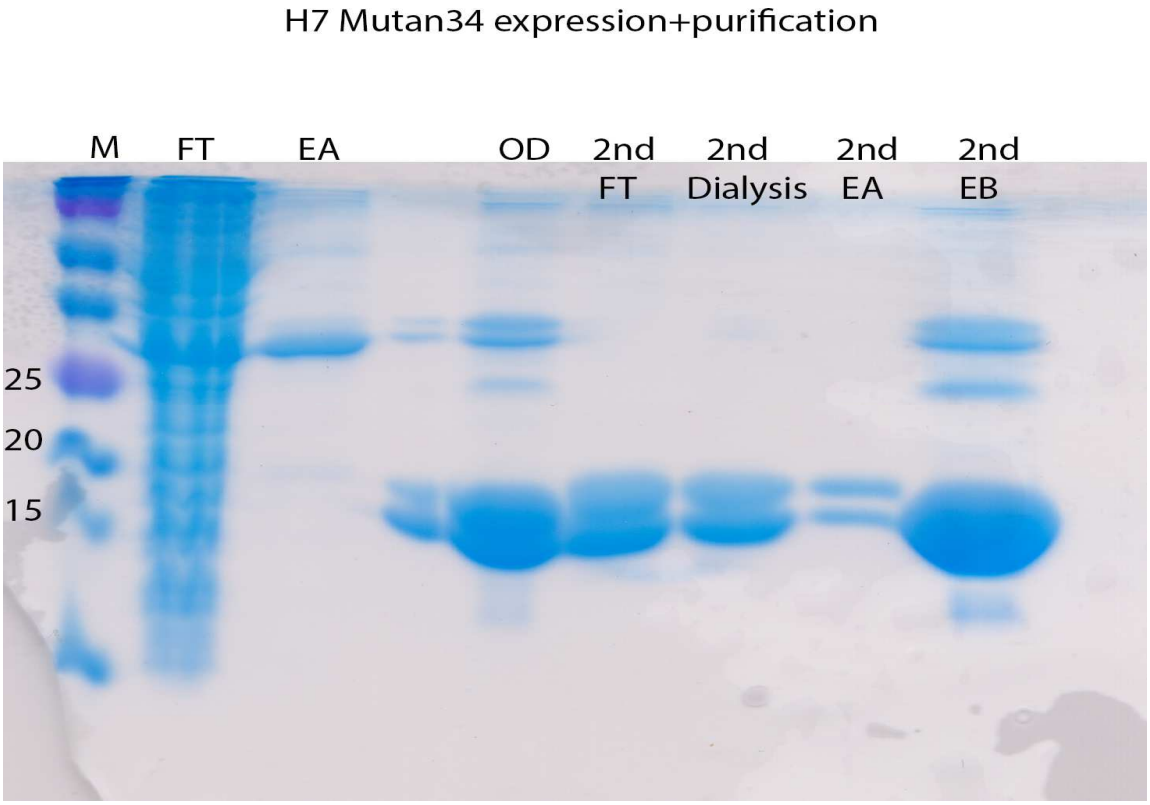

Figure3.7 4-Litter H7 SUMO construct expression and 2-Step Ni-NTA purification.

("M" refers to protein marker; "FT" refers to flow through sample; "EA" refers to buffer A elution sample; "OD" refers to overnight dialysis sample; "EB" refers to buffer B elution sample.)

From the SDS-PAGE gel's result, we collected sample from the 2nd FT to do further purification. High-load 75 column in AKTA HPLC equipment was used for the further purification, with the chromatograph shown in Fig. 3.8.

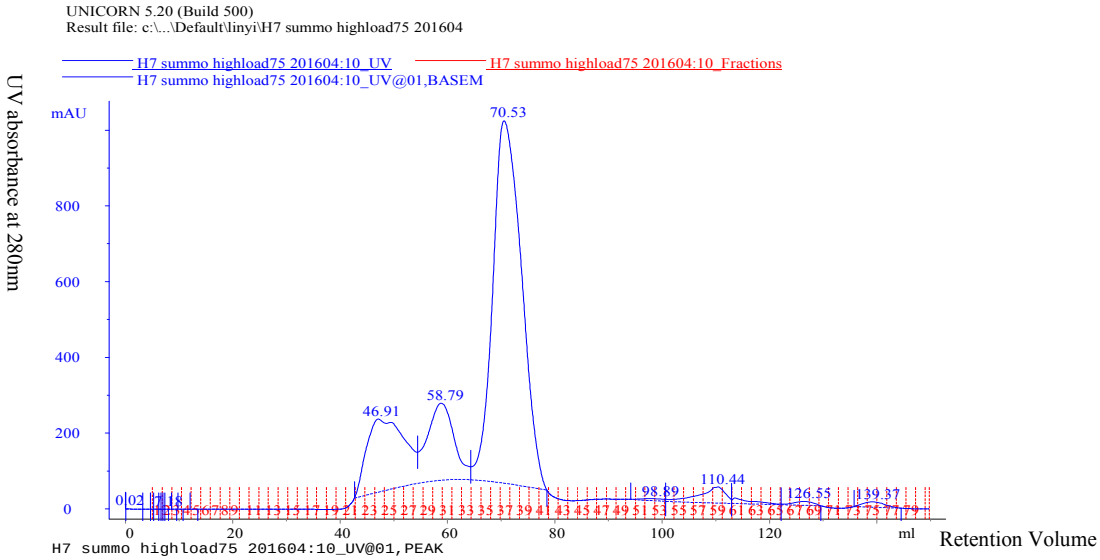

Figure 3.8 Gel filtration chromatograph of FL H7 using high-load superdex 75 column

To verify the proteins contained in each peak, a 15% SDS-PAGE gel was applied. The result of the SDS-PAGE gel is as followed:

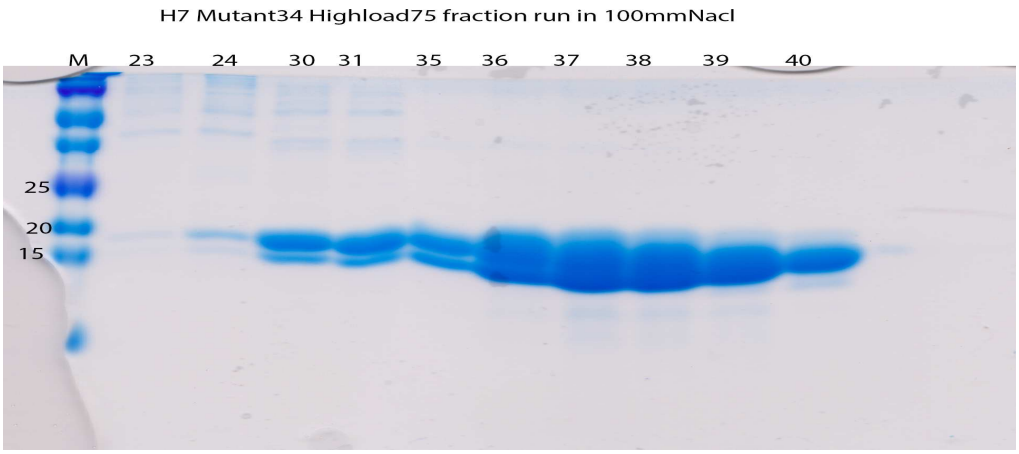

Figure 3.9 SDS-PAGE analysis of the fractions collected from gel filtration.

("M" refers to the protein marker; Fraction 23 to 24 refers to the far left peak; Fraction 30 to 31 refers to the middle peak; Fraction 35 to 40 refers to the far right peak.)

From the SDS-PAGE gel's result on the H7 SUMO construct's Highload 75 chromatography, we collected fraction 35 to 40 of which bands molecular weight are close to 17 k Da to do some further purification by ion exchange purification. Considering the H7 protein and SUMO protein's PI, a sepharose Q anion exchange column was used with Tris-buffer at pH 8.0. The result from the Q column ion exchange purification is shown in Fig. 3.10.

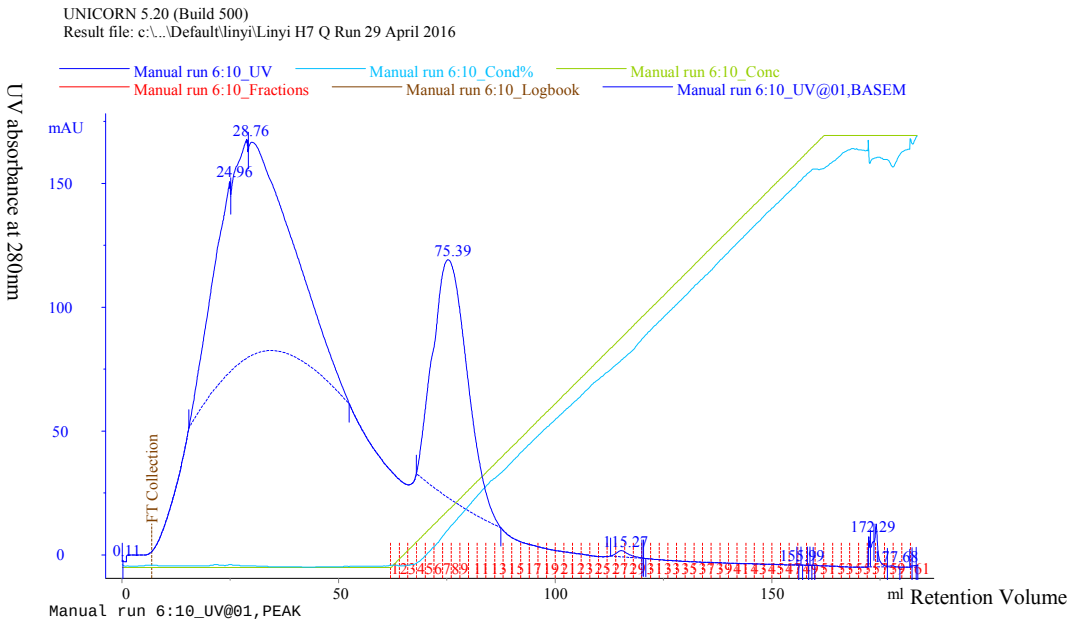

Figure 3.10 Ion exchange purification of FL H7

From the ion exchange chromatography, there are majorly two peaks appeared. The first peak that appears was the flow-through peak containing samples that did not bind with the ion exchange column. The second peak that followed the first peak contains proteins that eluted with the gradually increasing salt concentration. To verify the contents of the peak appeared on the chromatography, a 15% SDS-PAGE gel was applied. The SDS-PAGE gel result on this is presenting as followed:

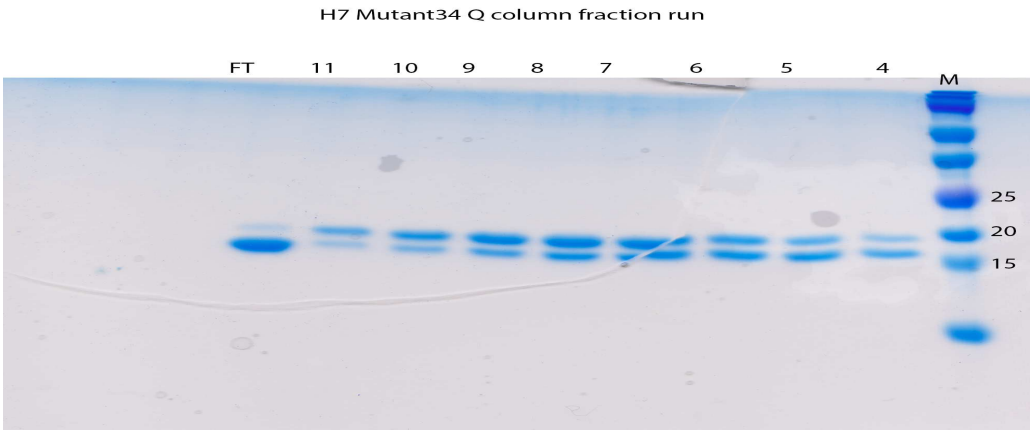

Figure 3.11 SDS-PAGE analysis of H7 protein from ion exchange chromatography.

("M refers to the protein marker"; "FT" refers to flow through which is the far left peak appeared on the chromatography; Fraction 4 to 11 refers to the second peak appeared on the chromatography)

From the 15% SDS-PAGE gel analysis on the Q column purification of H7, it is noticed that FT sample contains the target protein --H7. The purified H7 protein was concentrated to around 16mg/ml in 20 mM Tris, 50mM NaCl, flash frozen in LN2 and stored at -80 ℃ until usage for crystallization and lipid binding overlay assay. SDS-PAGE was used to test the purity of the final product. The result is presenting as followed:

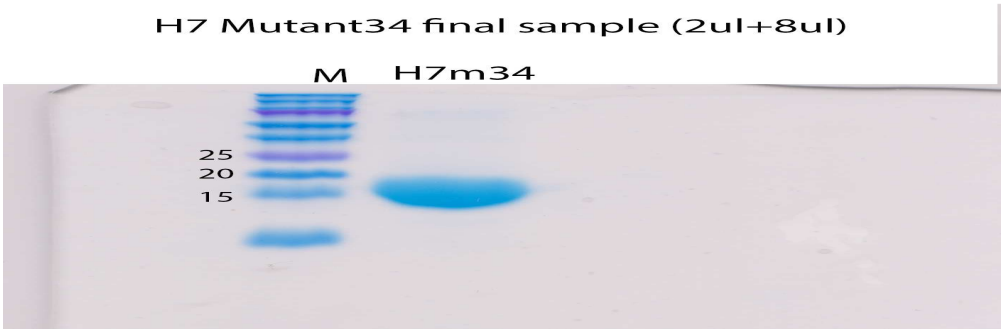

Figure 3.12 SDS-PAGE analysis of H7 final product.

("M" refers to the protein marker;)

III.3 Lipid Overlay Assay

III.3.1 BamB-H7 with Lipids

Purified BamB-H7 protein was diluted to 1ug/ml in 3% BSA, TBST buffer for the lipid overlay assay. The 1st anti-mouse polyclone antibody was used at 1:1000 dilution ratios. The 2nd anti-mouse HRP conjugated antibody was used at 1:2000 dilution ratios. The result of the lipid overlay assay using BamB-H7 fusion is presented in Fig. 3.13.

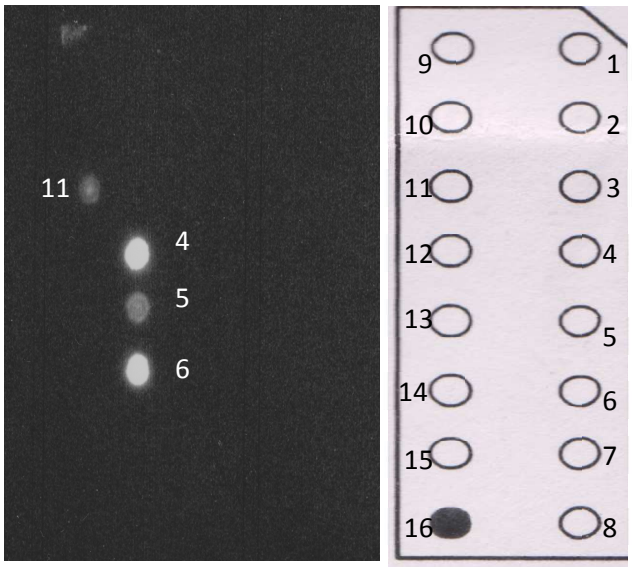

1:Lysophosphatidic Acid
2:Lysophosphocholine
3:Phosphatidylinositol
4:PI3P
5:PI4P
6:PI5P
7:Phosphatidylethanolamine
8:Phosphatidylcholine
9:Sphingosine-1-phosphate (S1P)
10:$PI(3,4)P_2$
11:$PI(3,5)P_2$
12:$PI(4,5)P_2$
13:$PI(3,4,5)P_3$
14:Phosphatidic Acid
15:Phosphatidylserine
16:Blank

Figure 3.13 Lipid overlay assay of BamB-H7

100-pmol spots of 15 different lipids are spotted on certain places at the nitrocellulous strip .The light spots in Figure 3.13 are the lipid- bound H7 protein detected by chemiluminescence with anti-H7 antibody.

It shows from the lipid overlay assay that the BamB-H7 binds with PI3P, PI4P, PI5P and $PI(3,5)P_2$.

III.3.2 FL H7 with Lipids

The lipid-binding assay was carried out in the same way as described above in III.3.1.

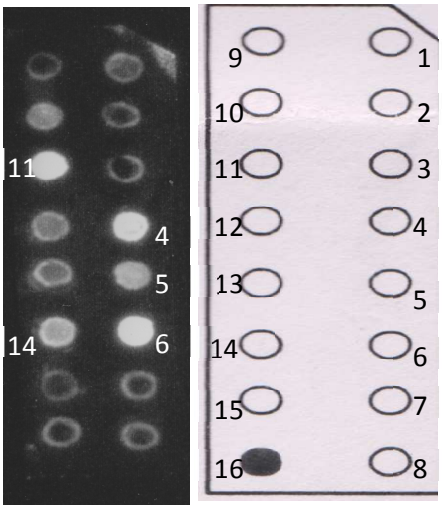

1:Lysophosphatidic Acid
2:Lysophosphocholine
3:Phosphatidylinositol
4:PI3P
5:PI4P
6:PI5P
7:Phosphatidylethanolamine
8:Phosphatidylcholine
9:Sphingosine-1-phosphate (S1P)
10:$PI(3,4)P_2$
11:$PI(3,5)P_2$
12:$PI(4,5)P_2$
13:$PI(3,4,5)P_3$
14:Phosphatidic Acid
15:Phosphatidylserine
16:Blank

Figure 3.14 Lipid overlay assay of H7 full length

Comparing the membrane with the template provided by the company, H7 binds with PI3P,PI4P,PI5P,$PI(3,5)P_2$ and PA. Note the lipid binding result is not exactly the same comparing to the published paper(Kolli et al., 2015).

III.4 Crystallization of H7 with Lipids

From the lipid overlay assay, the PI3P and PI4P's binding result is consistence with the previous studies (Kolli et al., 2015). Thus, at this stage, PI3P and PI4P were used to set up the H7-lipid co-crystallization for both purified FLH7 and BamB-H7 fusion proteins.

Among all the screening conditions (listed in Table 4), needle-like crystals from H7-PI3P complex formed in:

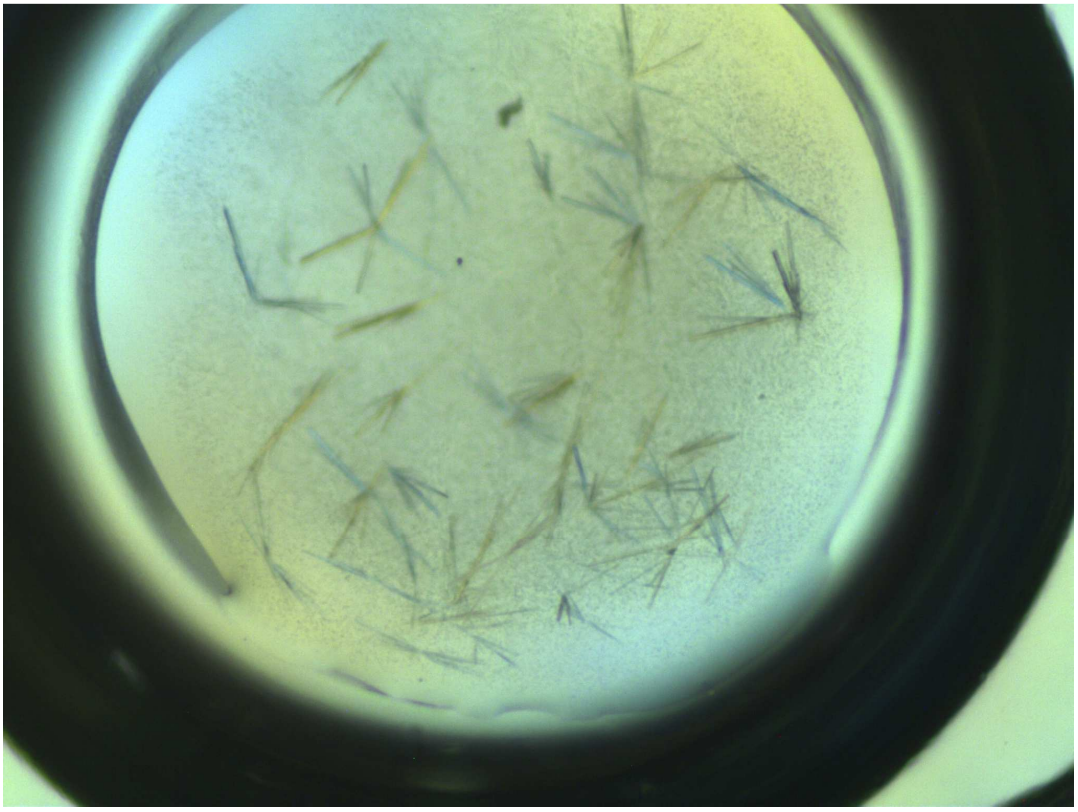

Figure **3.15** H7-PI3P complex crystal in H11, PEG/Ion II

1% w/v Tryptone, 0.05M HEPES sodium pH7.0, 12% w/v Polythylene glycol 3,350

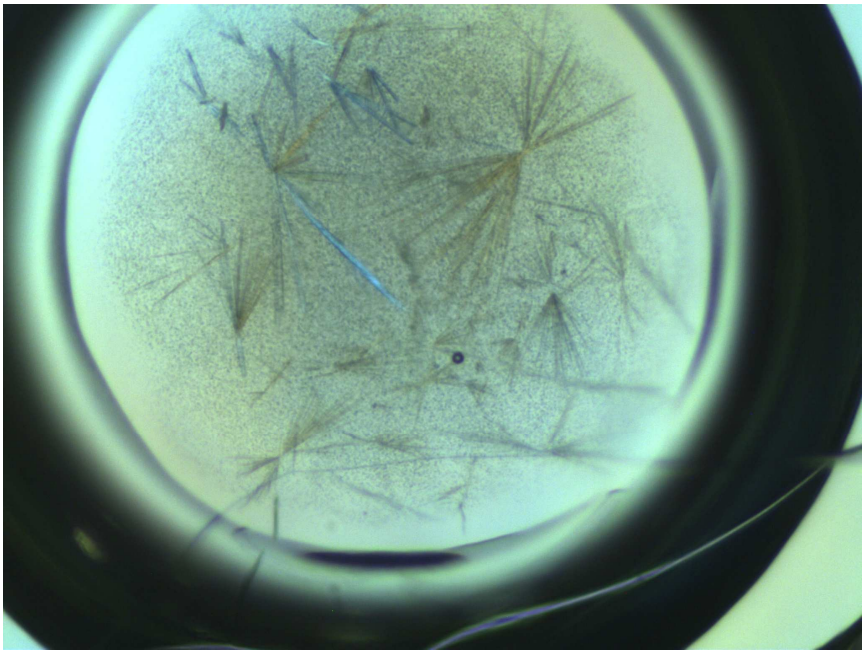

Figure **3.16** H7-PI3P complex crystal in H12, PEG/Ion II

1% w/v Tryptone, 0.05M HEPEs sodium pH 7.0, 20% w/v polyethylene glycol 3,350.

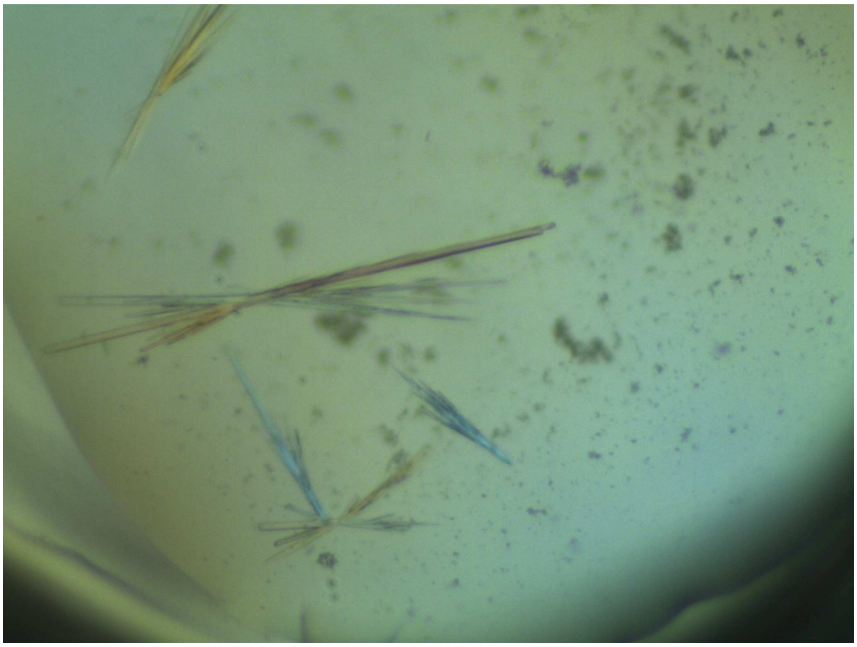

Figure **3.17** H7-PI3P complex crystal in H5, PEG/Ion II

(0.02M Citric acid, 0.05M BIS-TRIS protpane/pH 8.8), 16% w/v polyethylene glycol 3,350.

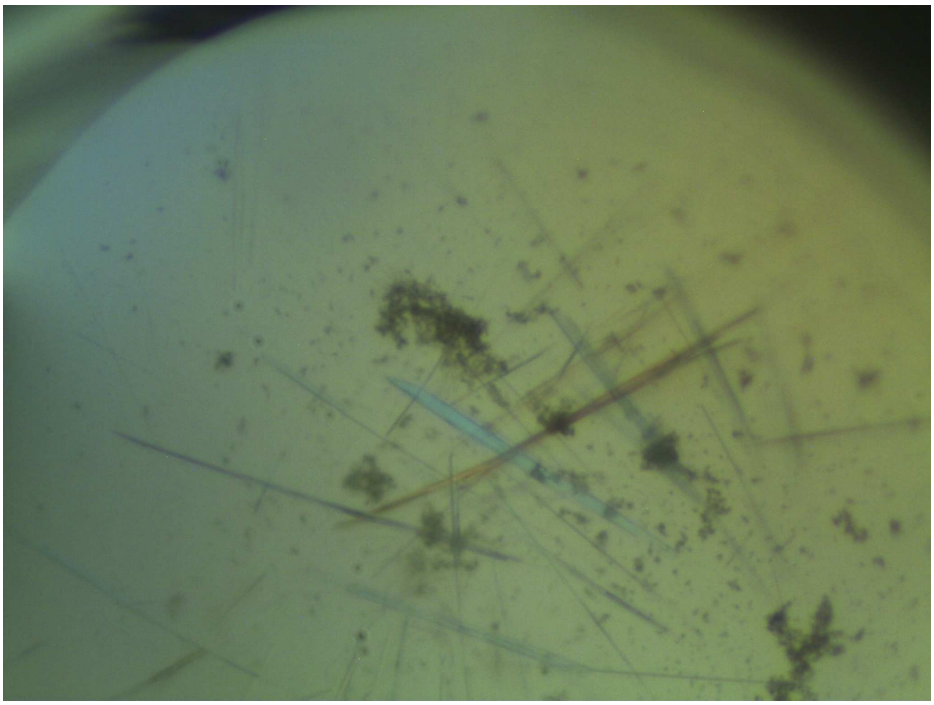

Figure **3.18** H7-PI3P complex crystal in G11, PEG/ION II

2% v/v Tacsimate pH 8.0, 0.1 M Tris pH 8.5, 16% w/v Polythylene glycol 3,350.

CHAPTER V

CONCLUSIONS

In this study, both H7's BamB and Sumo constructs have been successfully expressed and purified to homogeneous status.

The BamB-H7 construct's final product is BamB-H7 fusion protein. BamB is part of the outer membrane protein assembly Bam complex (Jansen et al., 2015; Wu et al., 2005), which crystallized in multiple forms. We hypothesized the fusion of BamB-H7 will yield various crystals forms, some of which may diffract to higher resolution. To exclude the possibility that the BamB moiety might block the lipid-binding site on H7, lipid-binding assay was conducted. The result of the BamB-H7 lipid binding assay shows that BamB-H7 indeed binds with several lipids including PI3P, PI4P, P15P and PI(3,5)P. The intensities of the spots on the PIP sheet correlate with binding affinity. It seems like that BamB-H7 has binds stronger with PI3P and PI5P. To verify this result, more repetitive experiments on this need to be carry out in the future.

The H7 SUMO construct's final product used for setting up crystallization is H7 itself. In this case, SUMO was used to facilitate the expression and purification of the protein of interest.

This SUMO construct was also used in the previous study(Kolli et al., 2015) to solve the crystal structure of H7 itself. It was also mentioned in the published paper that H7 used in solving the structure is a mutant with a C to S mutation at the position of the 89th amino acid. The mutant was used to disrupt the non-specific intermolecular disulfide bond thus improving the quality of the crystal. In this study, we used this construct to form a lipid complex for crystallization aim to solve the complete structure of H7.One thing caught our notice of this construct is that, the lipid binding assay had some different outputs from the published data (Kolli et al., 2015). Except PI3P and PI4P, a few other lipids also showed binding affinity in this study. This various unspecific binding specificity might due to the 3% BSA blocking buffer used in this study was not fatty acid free, which in some cases, might cause different binding pattern. Also, when using chemiluminescent method in the final detect step, exposure time also contributes to various out put. To verify the lipid binding result, more experiments with optimized buffer and exposure time at the last detect step need to be conducted in the future.

The needle-like crystals formed in this study need further optimization for better crystals before proceeding to the X-ray crystallography.

The structure-function study of H7 with lipid will verify the model proposed in our previous published paper (Kolli et al., 2015) and can provide us more clues in understanding the exact role of H7 and how it works with other VMAPs in the process of poxvirus viral membrane biogenesis.

REFERENCES

Amara, A., & Mercer, J. (2015). Viral apoptotic mimicry. *Nat Rev Microbiol, 13*(8), 461-469. doi:10.1038/nrmicro3469

Chlanda, P., Carbajal, M. A., Cyrklaff, M., Griffiths, G., & Krijnse-Locker, J. (2009). Membrane Rupture Generates Single Open Membrane Sheets during Vaccinia Virus Assembly. *Cell Host & Microbe, 6*(1), 81-90. doi:http://dx.doi.org/10.1016/j.chom.2009.05.021

Condit, R. C., Moussatche, N., & Traktman, P. (2006). In A Nutshell: Structure and Assembly of the Vaccinia Virion. *66*, 31-124. doi:10.1016/s0065-3527(06)66002-8

Dales S Fau - Mosbach, E. H., & Mosbach, E. H. (1968). Vaccinia as a model for membrane biogenesis. (0042-6822 (Print)).

Damon, I., Jahrling, P., & LeDuc, J. (2004). Poxviruses *Principles and Practice of Clinical Virology* (pp. 491-507): John Wiley & Sons, Ltd.

Delang, L., Paeshuyse, J., & Neyts, J. (2012). The role of phosphatidylinositol 4-kinases and phosphatidylinositol 4-phosphate during viral replication. *Biochem Pharmacol, 84*(11), 1400-1408. doi:10.1016/j.bcp.2012.07.034

Di Paolo, G., & De Camilli, P. (2006). Phosphoinositides in cell regulation and membrane dynamics. *Nature, 443*(7112), 651-657. doi:10.1038/nature05185

Erlandson, K. J., Bisht, H., Weisberg, A. S., Hyun, S. I., Hansen, B. T., Fischer, E. R., . . . Moss, B. (2016). Poxviruses Encode a Reticulon-Like Protein that Promotes Membrane Curvature. *Cell Rep, 14*(9), 2084-2091. doi:10.1016/j.celrep.2016.01.075

Heuser, J. (2005). Deep-etch EM reveals that the early poxvirus envelope is a single membrane bilayer stabilized by a geodetic "honeycomb" surface coat. *J Cell Biol, 169*(2), 269-283. doi:10.1083/jcb.200412169

Higashi, N., Ozaki, Y., & Ichimiya, M. (1960). Electron microscopy of pox virus-to-cell adsorption and the ultrastructure of developmental forms of pox virus. *Journal of Ultrastructure Research, 3*(3), 270-281. doi:http://dx.doi.org/10.1016/S0022-5320(60)80014-7

.

Amara, A., & Mercer, J. (2015). Viral apoptotic mimicry. *Nat Rev Microbiol, 13*(8), 461-469. doi:10.1038/nrmicro3469

Balla, T. (2013). Phosphoinositides: tiny lipids with giant impact on cell regulation. *Physiol Rev, 93*(3), 1019-1137. doi:10.1152/physrev.00028.2012

Chlanda, P., Carbajal, M. A., Cyrklaff, M., Griffiths, G., & Krijnse-Locker, J. (2009). Membrane Rupture Generates Single Open Membrane Sheets during Vaccinia Virus Assembly. *Cell Host & Microbe, 6*(1), 81-90. doi:http://dx.doi.org/10.1016/j.chom.2009.05.021

Condit, R. C., Moussatche, N., & Traktman, P. (2006). In A Nutshell: Structure and Assembly of the Vaccinia Virion. *66*, 31-124. doi:10.1016/s0065-3527(06)66002-8

Dales S Fau - Mosbach, E. H., & Mosbach, E. H. (1968). Vaccinia as a model for membrane biogenesis. (0042-6822 (Print)).

Delang, L., Paeshuyse, J., & Neyts, J. (2012). The role of phosphatidylinositol 4-kinases and phosphatidylinositol 4-phosphate during viral replication. *Biochem Pharmacol, 84*(11), 1400-1408. doi:10.1016/j.bcp.2012.07.034

Di Paolo, G., & De Camilli, P. (2006). Phosphoinositides in cell regulation and membrane dynamics. *Nature, 443*(7112), 651-657. doi:10.1038/nature05185

Erlandson, K. J., Bisht, H., Weisberg, A. S., Hyun, S. I., Hansen, B. T., Fischer, E. R., . . . Moss, B. (2016). Poxviruses Encode a Reticulon-Like Protein that Promotes Membrane Curvature. *Cell Rep, 14*(9), 2084-2091. doi:10.1016/j.celrep.2016.01.075

Heuser, J. (2005). Deep-etch EM reveals that the early poxvirus envelope is a single membrane bilayer stabilized by a geodetic "honeycomb" surface coat. *J Cell Biol, 169*(2), 269-283. doi:10.1083/jcb.200412169

Higashi, N., Ozaki, Y., & Ichimiya, M. (1960). Electron microscopy of pox virus-to-cell adsorption and the ultrastructure of developmental forms of pox virus. *Journal of Ultrastructure Research, 3*(3), 270-281. doi:http://dx.doi.org/10.1016/S0022-5320(60)80014-7

Husain, M., Weisberg As Fau - Moss, B., & Moss, B. (2006). Existence of an operative pathway from the endoplasmic reticulum to the immature poxvirus membrane. (0027-8424 (Print)). doi:D - NLM: PMC1681353 EDAT- 2006/12/06 09:00 MHDA- 2007/03/03 09:00 CRDT- 2006/12/06 09:00 PHST- 2006/12/04 [aheadofprint] AID - 0609406103 [pii] AID - 10.1073/pnas.0609406103 [doi] PST - ppublish

Jansen, K. B., Baker, S. L., & Sousa, M. C. (2015). Crystal structure of BamB bound to a periplasmic domain fragment of BamA, the central component of the beta-barrel assembly machine. *J Biol Chem, 290*(4), 2126-2136. doi:10.1074/jbc.M114.584524

Kolli, S., Meng, X., Wu, X., Shengjuler, D., Cameron, C. E., Xiang, Y., & Deng, J. (2015). Structure-function analysis of vaccinia virus H7 protein reveals a novel phosphoinositide binding fold essential for poxvirus replication. *J Virol, 89*(4), 2209-2219. doi:10.1128/JVI.03073-14

Krijnse Locker, J., Chlanda, P., Sachsenheimer, T., & Brugger, B. (2013). Poxvirus membrane biogenesis: rupture not disruption. *Cell Microbiol, 15*(2), 190-199. doi:10.1111/cmi.12072

Liem, J., & Liu, J. (2016). Stress Beyond Translation: Poxviruses and More. *Viruses, 8*(6). doi:10.3390/v8060169

Liu, L., Cooper, T., Howley, P. M., & Hayball, J. D. (2014). From crescent to mature virion: vaccinia virus assembly and maturation. *Viruses, 6*(10), 3787-3808. doi:10.3390/v6103787

Liu, L., Xu, Z., Fuhlbrigge, R. C., Pena-Cruz, V., Lieberman, J., & Kupper, T. S. (2005). Vaccinia virus induces strong immunoregulatory cytokine production in healthy human epidermal keratinocytes: a novel strategy for immune evasion. *J Virol, 79*(12), 7363-7370. doi:10.1128/JVI.79.12.7363-7370.2005

Lorizate, M., & Krausslich, H. G. (2011). Role of lipids in virus replication. *Cold Spring Harb Perspect Biol, 3*(10), a004820. doi:10.1101/cshperspect.a004820

Maruri-Avidal, L., Weisberg, A. S., & Moss, B. (2011). Vaccinia virus L2 protein associates with the endoplasmic reticulum near the growing edge of crescent precursors of immature virions and stabilizes a subset of viral membrane proteins. *J Virol, 85*(23), 12431-12441. doi:10.1128/JVI.05573-11

McFadden, G. (2005). Poxvirus tropism. *Nat Rev Microbiol, 3*(3), 201-213. doi:10.1038/nrmicro1099

McNulty, S., Bornmann, W., Schriewer, J., Werner, C., Smith, S. K., Olson, V. A., . . . Kalman, D. (2010). Multiple phosphatidylinositol 3-kinases regulate vaccinia virus morphogenesis. *PLoS One, 5*(5), e10884. doi:10.1371/journal.pone.0010884

Meng, X., Wu, X., Yan, B., Deng, J., & Xiang, Y. (2013). Analysis of the role of vaccinia virus H7 in virion membrane biogenesis with an H7-deletion mutant. *J Virol, 87*(14), 8247-8253. doi:10.1128/JVI.00845-13

Moss, B. (2015). Poxvirus membrane biogenesis. *Virology, 479-480*, 619-626. doi:10.1016/j.virol.2015.02.003

Roberts, K. L., & Smith, G. L. (2008). Vaccinia virus morphogenesis and dissemination. *Trends Microbiol, 16*(10), 472-479. doi:10.1016/j.tim.2008.07.009

Satheshkumar, P. S., Weisberg, A., & Moss, B. (2009). Vaccinia virus H7 protein contributes to the formation of crescent membrane precursors of immature virions. *J Virol, 83*(17), 8439-8450. doi:10.1128/JVI.00877-09

Schramm, B., & Locker, J. K. (2005). Cytoplasmic organization of POXvirus DNA replication. *Traffic, 6*(10), 839-846. doi:10.1111/j.1600-0854.2005.00324.x

Stenmark, H., & Gillooly, D. J. (2001). Intracellular trafficking and turnover of phosphatidylinositol 3-phosphate. *Semin Cell Dev Biol, 12*(2), 193-199. doi:10.1006/scdb.2000.0236

Szajner, P., Weisberg, A. S., Lebowitz, J., Heuser, J., & Moss, B. (2005). External scaffold of spherical immature poxvirus particles is made of protein trimers, forming a honeycomb lattice. *The Journal of Cell Biology, 170*(6), 971-981. doi:10.1083/jcb.200504026

Ward, B. M., & Moss, B. (2001). Vaccinia virus intracellular movement is associated with microtubules and independent of actin tails. *J Virol, 75*(23), 11651-11663. doi:10.1128/JVI.75.23.11651-11663.2001

Wlodawer, A., Minor, W., Dauter, Z., & Jaskolski, M. (2008). Protein crystallography for non-crystallographers, or how to get the best (but not more) from published macromolecular structures. *FEBS J, 275*(1), 1-21. doi:10.1111/j.1742-4658.2007.06178.x

Wu, T., Malinverni, J., Ruiz, N., Kim, S., Silhavy, T. J., & Kahne, D. (2005). Identification of a multicomponent complex required for outer membrane biogenesis in Escherichia coli. *Cell, 121*(2), 235-245. doi:10.1016/j.cell.2005.02.015

APPENDICES

Abbreviations

AKT……Protein Kinase B
BSA……Bovine Serum Albumin
ER……....Endoplasmic Reticulum
EV……..Enveloped Virion
IMV……Intracellular Mature Virion
IPTG……Isopropyl β-D-1-thiogalactopyranoside
MT……..Microtubule
MV……...Mature Viron
NI-NTA……Nickle-Nitrilotriacetic acid
PIP……..Phosphoinositide
PI3P…….....Phosphatidylinositol 3-phosphate
PI4P……..Phosphatidylinositol 3-phosphate

VITA

LINYI TANG

Candidate for the Degree of

Master of Science

Thesis: STRUCTURE FUNCTION STUDIES ON A LIPID BINDING PROTEIN H7 FROM VACCINIA VIRUS.

Major Field: Protein Structure Study

Biographical:

Education:

Completed the requirements for the Master of Science in Biochemistry and Molecular Biology at Oklahoma State University, Stillwater, Oklahoma in July, 2016.

Completed the requirements for the Bachelor of Science in Biology Science at South China Normal University, Guangzhou, China in 2010.